

The Effect of Cyclic Loading on the Mechanical Performance of Surgical Mesh

S. M. Patterson¹, Y. C. Ho², W. C. Wang²

¹Department of Engineering Science, University of Oxford, Oxford, United Kingdom

²Department of Power Mechanical Engineering, National Tsing Hua University, Hsinchu, Taiwan, Republic of China

ABSTRACT

Polymeric meshes in the form of knitted nets are commonly used in the surgical repair of pelvic organ prolapses. Although a number of these prosthetic meshes are commercially available, there is little published data on their mechanical performance, in particular on the change in stiffness under the repeated loading experienced *in vivo*. In this *in vitro* study, cyclic tensile loading was applied to rectangular strips of four different commercially available meshes. The applied force and resultant displacement was monitored throughout the tests in order to evaluate the change in stiffness. In addition, each mesh was randomly marked using indelible ink in order to permit the use of three-dimensional digital image correlation to evaluate local displacements during the tests. However, the scale and form of the deformation experienced by some of the meshes made correlation difficult so that confirmation of the values of stiffness were only obtained for two meshes. The results demonstrate that all the meshes experience an increase in stiffness during cyclic loading, that in most cases cyclic creep occurs and in some cases large-scale, irreversible reorganisation of the mesh structure occurs after as few as 200 cycles at loads of the order of 10N.

INTRODUCTION

Surgically implanted artificial mesh is commonly used in the treatment of pelvic organ prolapse [1]. Pelvic Organ Prolapse is a condition affecting women during menopause and those who have given birth vaginally [2]. The condition is caused by a weakened pelvic floor which leads to the pelvic organs moving and falling on to the vagina, resulting in considerable discomfort to the patient [2]. One possible treatment is to use artificial mesh to reinforce the pelvic floor and help hold the organs in place. However, little is known about the mechanical properties of such artificial meshes. Previous work investigated the performance of artificial meshes subject to static tension loading [3]. The aim of this paper is to understand the behaviour and properties of the artificial mesh under cyclic loading.

Digital Image Correlation (DIC) is a non-contact technique used for measuring displacement from which motion and strain can be deduced. The technique relies on small-scale high contrast features randomly present in images of the specimen. Before a test is carried out, an initial reference image is taken of the specimen and a subset is defined. Images are taken at regular intervals throughout the test by CCD cameras that are connected to DIC software. The software tracks the displacement of the speckles in the subset and uses a least squares algorithm to calculate displacement. Then strain can be calculated using the displacement gradient. To measure out-of-plane displacement,

two CCD cameras and a 3D DIC algorithm are required. The images captured by the two cameras are combined using stereo triangulation that requires an initial calibration. 3D DIC is used in this experiment to measure the deformation of four types of artificial mesh during fatigue tests.

EXPERIMENTAL PROCEDURE

Four types of artificial mesh used in the repair of pelvic organ prolapse were tested, namely Bard Soft (Bard, Murray Hill, NJ), Gynemesh (Genecare, Chapel Hill, NC), Marlex (Bard, Murray Hill, NJ) and Mersilene (Ethicon, Cornelia, GA). The artificial mesh specimens measured 45mm in the direction the loading and 20mm in width. The samples were cut from a larger roll of mesh in such a way as to avoid including any irregularities at the edge of the roll and so that loading was only applied along the axis of knitting. Prior to the tests, the specimens were prepared for analysis using DIC by applying a powder to the mesh in order to reduce glare and reflection that would cause errors in the analysis. Speckles were then randomly applied to the mesh using an extra fine black marker pen. Once the speckles had been applied, two rubber end tabs were fixed at each end of the specimen. Each pair of tabs was carefully glued together by putting drops of glue on the faces of the tabs to avoid the glue touching the mesh but to trap the end of the mesh between the tabs. The glue used was cyanoacrylate. The rubber tabs measured 10mm in the direction of tension and 20mm in width so that the gauge length of the artificial mesh was 25mm. The tabs prevented the mesh slipping in the clamps of the tensile machine and provided a more uniform transfer of load, thus reducing potential errors.

The mesh specimens with the rubber tabs fitted at each end were loaded in a Instron 8848 micro-tensile test machine [3] at a displacement rate of 30mm/min for 200 cycles with a maximum load of 10N. During the tests images were captured every four seconds using two high resolution (1628 pixel x 1236 pixel) CCD cameras. The images were processed using the VIC-3D systems (Correlated Solutions, Columbia, NC) to obtain displacements for selected areas of interest (20 x 25 mm) in the center portion of the gauge-section. Cross-head displacements and load values from the load cell on the test machine were also monitored so that engineering stress and strain could be calculated based on the original cross-section area and gauge length of the specimen.

RESULTS AND DISCUSSION

Figure 1 shows the force-displacement graphs for each of the four meshes using the data from the tensile machine. There is a wide range in the performance with maximum displacements of 20.2mm, 6.67mm, 3.93mm and 2.6mm for Bard Soft, Gynemesh Marlex and Mersilene respectively. Stress and strain data were calculated from this data is shown in Fig. 2 for the first, tenth, hundredth, and two hundredth cycle of testing. Bard soft mesh was only tested up to 100 cycles because the deformation was so large (Fig. 3). The slight curvature in the graphs for some of the meshes probably is caused by slack in the system when the load is zero. In data in Fig. 2 indicates that the Young's modulus for all of the meshes increases with the number of cycles and that Mersilene has consistently the highest Young's modulus doubling from 30MPa in the first cycle to 60MPa in the 200th cycle. The modulus for Gynemesh almost tripled from 7MPa to 20MPa while for

Bard Soft it more than tripled in only 100 cycles from 2MPa to 7MPa. For Marlex the modulus changed the least from 6MPa in the first cycle to 9MPa in the 200th cycle.

Successful analysis of the tests using DIC was only achieved for the two meshes that exhibited the lowest levels of modulus change during the 200 cycles, i.e. Mersilene and Marlex. The deformation of Gynemesh and Bard Soft was too large and hence, the error from the DIC analysis was very high due to decorrelation because insufficient images were captured to define the deformation. The horizontal fibres of the mesh deformed vertically rather than horizontally and so a first order approximation of the deformation was not adequate to calculate the displacement [4]. Observation of the behaviour of Gynemesh and Bard Soft revealed that these meshes behaved more like a structure than a material, in other words the weave of the material breaks up so that there is no longer a continuum (see Fig. 3) making DIC analysis impossible at this scale. This behaviour could be explained by the large holes in Gynemesh and Bard Soft compared to Mersilene and Marlex in their initial state. Figure 4 shows the strain-time graphs for Marlex and Mersilene based on the DIC results. Instantaneous Young's moduli were calculated as the ratio of the gradient from these results and the gradient of the stress-time curves from the tensile machine data and are shown in Fig. 5 together with the data from Fig. 2 which is derived entirely from the test machine. Except for the Mersilene DIC results, Young's moduli increase significantly in the first few cycles and then remain essentially constant for the rest of the test. It is very obvious from Fig. 5 that the results obtained from DIC and tensile test for Marlex are in good agreement. For Mersilene the stiffness based on the DIC data was significantly less than the value obtained solely based on data from the test machine and also tended to be noisier. This is not unexpected because the data from DIC is taken from only on the area in the middle of the test sample and hence provides an assessment of the local stiffness rather than the gross stiffness obtained from the test machine data. In particular, in contrast to Fig. 3(h) for the case of Marlex after cyclic loading, necking phenomenon does occur for the case of Mersilene after cyclic loading (Fig. 3(f)). Nevertheless, the trends in the data are consistent between the two data sets with the Mersilene artificial mesh exhibiting the highest stiffness and thus potentially providing the best prognosis for treatment.

CONCLUSION

In this study, the cyclic loading of surgical mesh was analysed using displacement data from both cross-head of the tensile machine and from 3D DIC. DIC analysis was unsuccessful for two of the four materials examined because the deformations were so large and the meshes had a very open weave and so behaved as a structure rather than a continuum material. Stiffness data was calculated as a function of time (no. of cycles) and initially increased steeply. The Young's modulus obtained from DIC agrees well with that obtained from the tensile test. However, because of the necking phenomenon, the local stiffness data based on the strain data obtained from DIC for the Mersilene was rather lower and noisier than that based on the strain data obtained from cross-head displacements. Based on the results presented in this paper, the too large deformation occurred in Gynemesh and Bard Soft as well as the necking phenomenon happened to the Mersilene could be avoided by applying lower load.

The results indicate that Mersilene should be the preferred mesh for use in surgery because it exhibits the lowest level of deformation and has the highest stiffness. To confirm this conclusion, further tests could be carried out at in vivo temperatures and the meshes could be tested on the cross knitting axis.

Acknowledgments

This research was supported in part by the National Science Council (grant no. NSC95-2221-E007-011-MY3), Taiwan, Republic of China. Summer internship scholarship provided by the Department of Power Mechanical Engineering of the National Tsing Hua University to Sarah Patterson is also greatly appreciated.

References

- [1] <http://www.pelvichealthsolutions.com/pelvic-organ-prolapse>
- [2] <http://www.instron.com.tw/>
- [3] Wang, W. C., Yu, K. J., Chu, T. P., Shen, H. T., Chang, T. Y., Measurement of Mechanical Properties and Deformation of Artificial Mesh by Digital Image Correlation Method, Proc. SEM Annual Conference & Exposition on Experimental and Applied Mechanics, paper no. 172, 9 pages, Albuquerque, NM, USA, June 2009.
- [4] Lu, H/ and Cary, P. D. (2000) Deformation Measurements by Digital Image Correlation: Implementation of a Second-order Displacement Gradient. *Experimental Mechanics*. 40:4 pg 393-400.

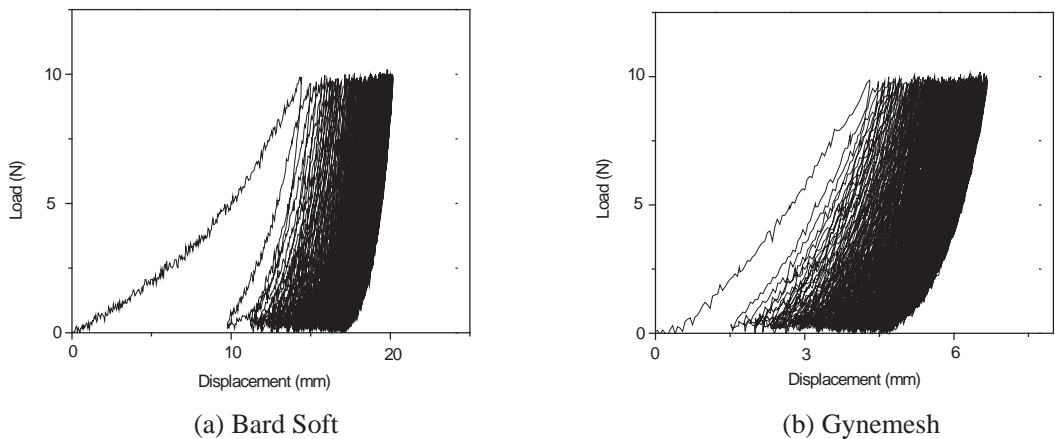
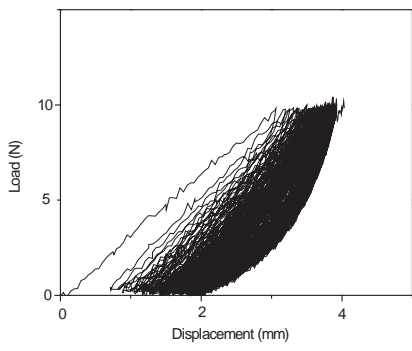
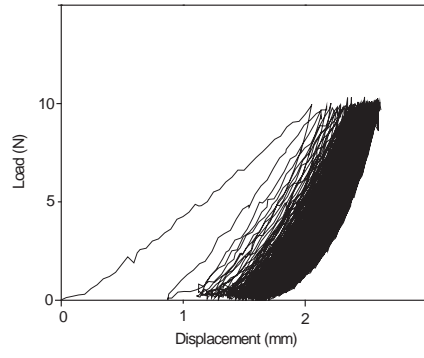


Fig. 1 Force-displacement graphs for four types of artificial mesh using tensile machine data.

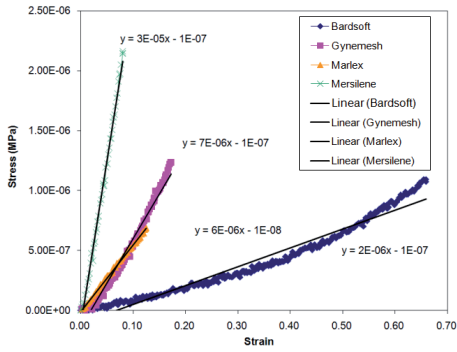


(c) Marlex

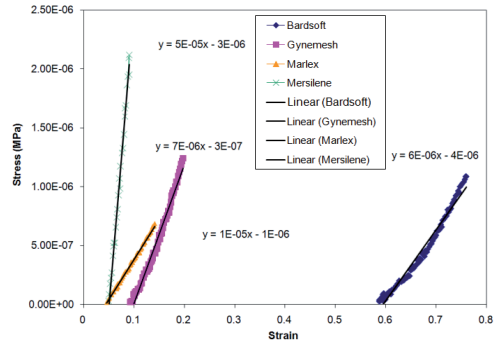


(d) Mersilene

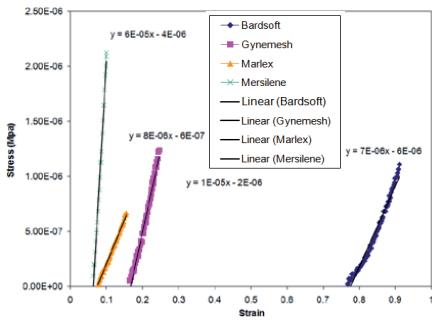
Fig. 1 (Continued)



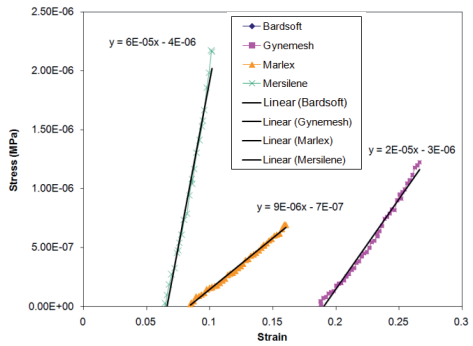
(a) First cycle



(b) 10th cycle

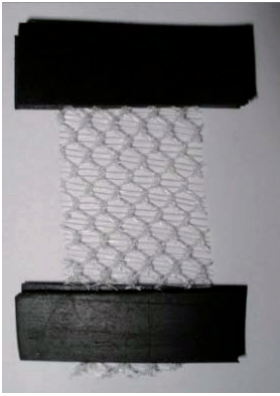


(c) 100th cycle

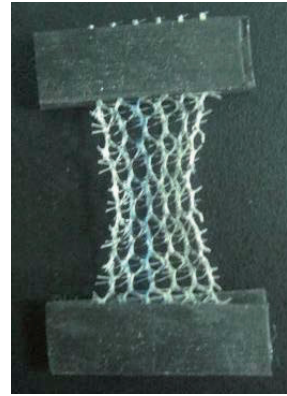


(d) 200th cycle

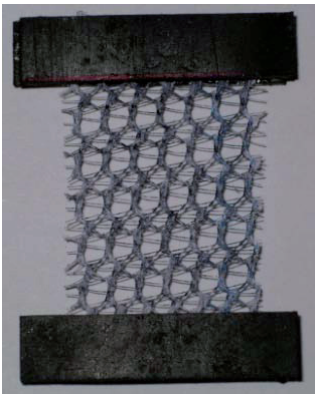
Fig. 2 Stress-strain data based on the cross-head displacement and load cell data from the test machine.



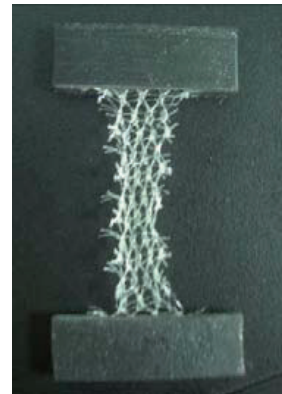
(a) Bard Soft before



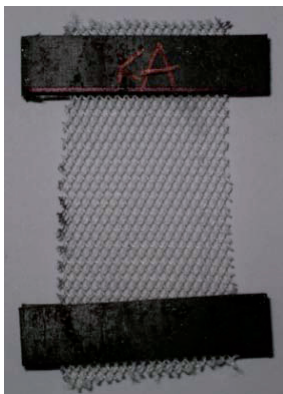
(b) Bard Soft after



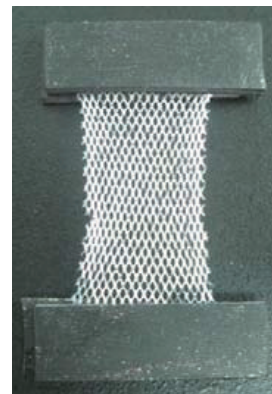
(c) Gynemesh before



(d) Gynemesh after

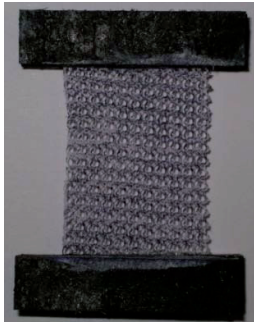


(e) Mersilene before

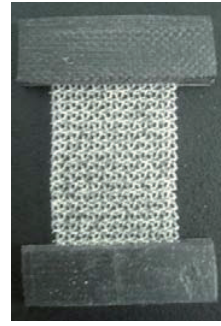


(f) Mersilene after

Fig. 3 Images of the mesh before and after cyclic loading

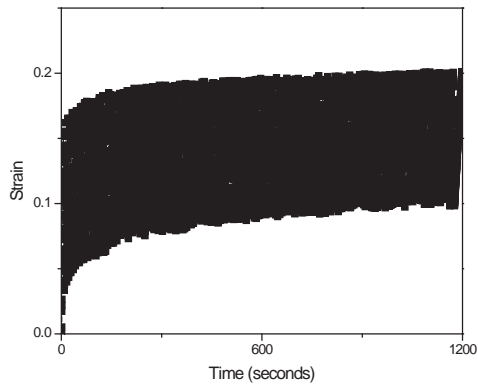


(g) Marlex before

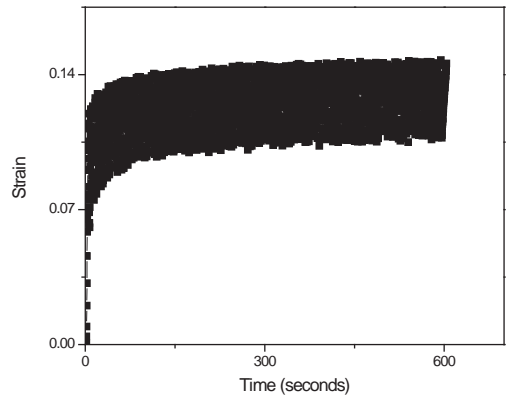


(h) Marlex after

Fig. 3 (Continued)



(a) Marlex



(b) Mersilene

Fig. 4 Strain-time plots based on DIC data.

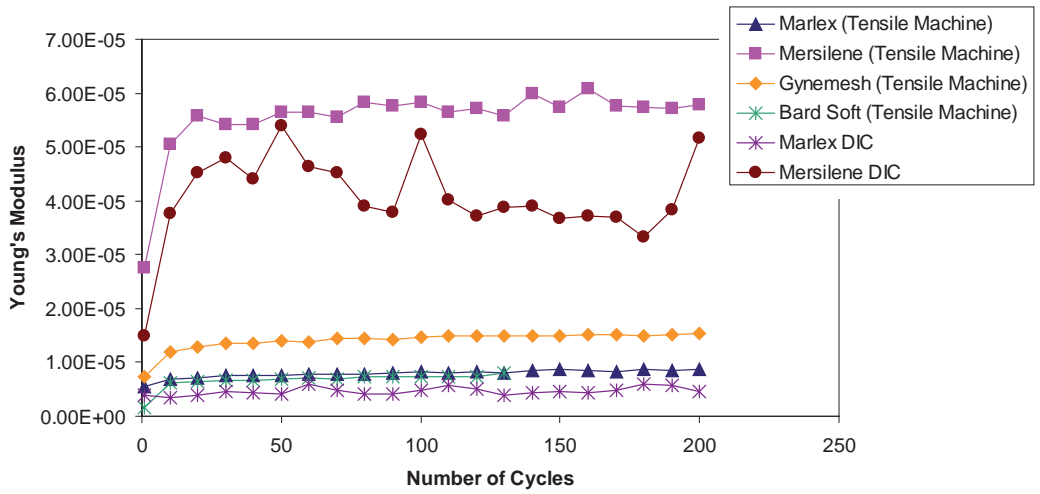


Fig. 5 Young's modulus as function of number of cycles based on data from the tensile machine and DIC.